

Femtosecond Optical Responses of Disordered Clusters, Composites, and Rough Surfaces: “The Ninth Wave” Effect

Mark I. Stockman*

Department of Physics and Astronomy, Georgia State University, Atlanta, Georgia 30303

(Received 7 September 1999)

We predict that in the course of femtosecond excitation of random clusters, composites, or rough surfaces in the optically linear regime, ultrafast giant fluctuations of local fields occur. These fluctuations cause transient (on a femtosecond scale) formation of highly enhanced fields localized in nanometer-size regions (“the ninth wave effect”). The spatial distribution of those fields is dramatically different from the case of steady-state excitation. We discuss manifestations of this effect and possible experiments.

PACS numbers: 78.20.Bh, 42.65.Sf, 71.45.Gm, 78.47.+p

In this paper we consider ultrafast optical responses of strongly disordered systems (fractal clusters, rough surfaces, and random composites) whose size is mesoscopic, i.e., much larger than the atomic size but much smaller than the light wavelength. We predict from our computations that femtosecond linear responses of such systems show what we call “the ninth wave effect” [1]. Namely, in the course of evolution of the system induced by a femtosecond laser pulse, excitation initially spread over the whole system concentrates in a narrow (on a nanometer scale) region, where a local field develops that can exceed the average and exciting fields by orders of magnitude. The spatiotemporal behavior of the local fields is deterministically chaotic, i.e., random, but fully reproducible for the given system and the exciting pulse.

This effect is a dynamic counterpart of the chaoticity of the eigenmodes, their inhomogeneous localization, and giant spatial fluctuations of the local fields in random systems predicted earlier for steady-state excitation [2–4] and observed experimentally (see, e.g., Refs. [5,6], and citations therein). The femtosecond dynamics of the local field at the site of the maximum field (“hot spot”) is very different from that of the averaged field. The spatial distribution of the femtosecond local fields near the maximum-field time is very singular and localized, and dramatically different from the steady-state distribution.

Recently, great progress has been achieved in physics of femtosecond pulses [7–10] (see also references therein). Effects of intense femtosecond radiation include generation of high harmonics from the visible to x-ray region [7], strong x-ray emission from hot plasmas produced by irradiation of colloidal metals [11] and clusters in gases [12], and multiple ionization of metal clusters enhanced by plasmons [13]. Existence of radiation sources and the multitude of femtosecond effects shows feasibility and relevance of the phenomena predicted in this paper.

Quantitatively, consider a system consisting of N particles (monomers) positioned at coordinates \mathbf{r}_i , $i = 1, \dots, N$. The electric field of the exciting pulse at an i th monomer at time t , denoted $\mathbf{E}_i^{(0)}(t)$, is assumed to be non-saturating and known. We define a local field at this

monomer \mathbf{E}_i in terms of the corresponding induced dipole moment $\mathbf{d}_i(\omega) = \alpha_0(\omega)\mathbf{E}_i(\omega)$, where $\alpha_0(\omega)$ is the dipole polarizability of an isolated monomer at a frequency ω . Throughout the paper, we imply the Fourier (frequency) domain by simply indicating frequency arguments ω, \dots , as opposed to time variables t, t', \dots for the real time domain. In specific computations, we consider the monomers as spheres of radius R_m , for which $\alpha_0(\omega) = R_m^3[\epsilon(\omega) - 1]/[\epsilon(\omega) + 2]$, where $\epsilon(\omega)$ is the relative dielectric function of the monomer material.

The local field $\mathbf{E}_i(t)$ at a time t at an i th monomer is given by a retarded Green’s function of the system G^r ,

$$E_{i\beta}(t) = \sum_{j=1}^N \int_{-\infty}^t G_{i\beta,j\gamma}^r(t-t') E_{j\gamma}^{(0)}(t') dt'. \quad (1)$$

Here and below, Greek subscripts denote Cartesian components with summation over recurring indices implied.

To find G^r , we use two well-tested approximations. First, the quasistatic approximation implies that the size of the system is much smaller than the light wavelength and absorption depth. This excludes effects of light propagation, extinction, and formation of polaritons. However, the rich femtosecond dynamics is preserved, since it is due to motion of surface plasmons on subwavelength scale. The second is the dipole approximation that is applicable because the effects predicted are collective, formed by interactions of many monomers at distances $\gg R_m$. We use the dipolar spectral theory of Ref. [14] that is an approximation of the exact spectral theory [15].

In the dipole approximation, the local field problem reduces to a well-known set of coupled-dipole equations,

$$Z(\omega)d_{i\beta}(\omega) = E_{i\beta}^{(0)}(\omega) - \sum_{b=1}^N W_{\beta\gamma}(\mathbf{r}_i, \mathbf{r}_j) d_{j\gamma}(\omega), \quad (2)$$

where $Z(\omega) = \alpha_0^{-1}(\omega)$, and the dipole-interaction tensor is $W_{\beta\gamma}(\mathbf{r}, \mathbf{r}') = -\frac{\partial}{\partial r_\beta} \frac{\partial}{\partial r'_\gamma} \frac{1}{|\mathbf{r}-\mathbf{r}'|}$. We introduce $3N$ -dimensional vectors $|d\rangle$, $|E^{(0)}\rangle, \dots$ with the components $(i\beta|d) = d_{i\beta}$, $(i\beta|E^{(0)}) = E_{i\beta}^{(0)}$ (and similarly for other vectors), and obtain a single equation in a $3N$ -dimensional

space, $[Z(\omega) + W]|d(\omega)) = |E^{(0)}(\omega))$, where $(i\beta|W|j\gamma) = W_{\beta\gamma}(\mathbf{r}_i, \mathbf{r}_j)$ [14].

The solution of Eq. (2) is determined by the eigenvalues w_n and eigenvectors (eigenmodes) $|n\rangle$ of the stationary W operator, $(W - w_n)|n\rangle = 0$, where $n = 1, \dots, 3N$ is the eigenmode's number. These eigenmodes are the surface plasmons of the whole system. The required Green's function in the frequency representation is

$$G_{i\beta, j\gamma}^r(\omega) = Z(\omega) \sum_n (i\beta|n)(j\gamma|n)(Z(\omega) + w_n)^{-1}, \quad (3)$$

where $(i\beta|n)$ is an amplitude of an n th eigenmode at an i th monomer with polarization β .

We have carried out numerical computations for three types of random systems generated by the Monte Carlo method. Two of them are fractal clusters, namely cluster-cluster aggregates (CCA) [16,17] in two and three dimensions, and the third is random composites of spheres with fill factor $f = 0.12$. For definiteness, we assume that the monomers are silver nanospheres whose dielectric function is that of bulk silver [18]. For 3D CCA and for composites, we take the ambient medium to have a dielectric constant of 2.0, while for 2D CCA it is vacuum. The number of monomers in a cluster or in the composite's unit cell is set $N = 1500$. For composites, we impose periodic boundary conditions on the unit cell. We use a Gaussian shape with linear polarization for the exciting pulse with unit amplitude, carrier frequency ω_0 , and pulse length T , $E^{(0)}(t) = \cos(\omega_0 t) \exp(-t^2/T^2)$. For each system, ω_0 has been chosen near the absorption maximum.

We show in Fig. 1 the predicted femtosecond dynamics of induced electric fields for a three-dimensional (3D) CCA cluster (a fractal with Hausdorff dimension $D \approx 1.75$). Importantly, the local field E_{mz} at the site of its maximum ("hot spot") is enhanced by more than 2 orders of magnitude with respect to both the exciting field $E_z^{(0)}$ and the averaged local field $\langle E_{iz} \rangle$. The hot-spot field $E_{mz}(t)$ reaches its maximum by the end of the exciting pulse, which implies that the excitation process is coherent, occurring before relaxation runs its course. The mean-field dynamics exhibits pronounced coherent beats due to interference between different eigenmodes.

Since clusters under consideration are complicated chaotic many-body systems, they possess a hierarchy of characteristic times. The shortest of these times τ_ω determines the buildup of spikes of local fields. It is on the order of a period of contributing eigenmodes $\tau_\omega \approx 2\pi/\omega \approx 4$ fs. The temporal decay of those spikes is determined by much longer relaxation times $\tau_d(\omega)$. These can be found from Eq. (3) as $\tau_d = \frac{dX(\omega)}{d\omega}/\delta(\omega)$, where $X(\omega) \equiv -\text{Re}Z(\omega)$ and $\delta \equiv -\text{Im}Z(\omega)$ are spectral variables [14]. For $\omega = 0.8-1.2$ eV relevant for Fig. 1 and parameters of Ref. [18], $\tau_d = 55-72$ fs in agreement with the decay times of the hot-spot field E_{mz} in Fig. 1.

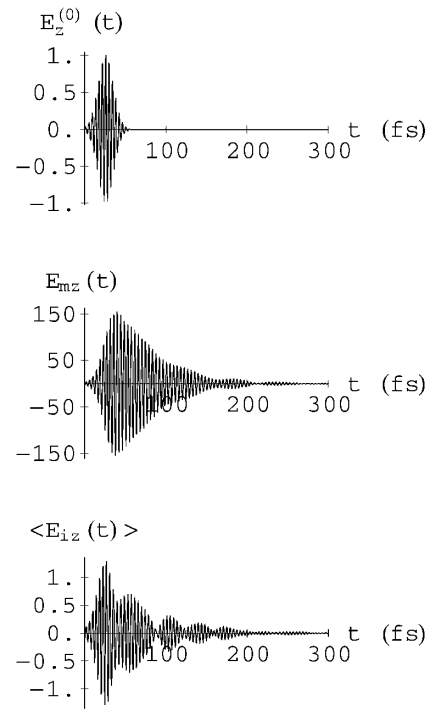


FIG. 1. For a 3d CCA cluster, dependencies on time of the exciting field $E_z^{(0)}(t)$, the local field (z polarization) at the site of the maximum field $E_{mz}(t)$, and the local field averaged over all monomers $\langle E_{iz}(t) \rangle$. The carrier frequency (in energy units) is 1.0 eV, and the pulse length is $T = 25$ fs.

The dynamics of the spatial distribution of local fields is shown in Fig. 2. At all times, the distributions are very chaotic and singular. After just a few oscillations of the driving pulse ($t = 6.4$ fs), the fields are excited nonselectively at most of the monomers, because such a short excitation acts as an instantaneous perturbation. In contrast, the development of a self-consistent polarization requires time $t \gg \tau_\omega$. In other terms, the initially excited surface plasmons have to move through the system to establish true eigenmodes, and there has not been enough time for that. In contrast, at the moment of "the ninth wave" $t = 40$ fs, there is a dominating hot spot with the electric field enhanced by a factor of ≥ 250 , while the rest of the system is weakly excited. This "ninth wave" persists long into the free-induction stage ($t = 92$ fs) where the exciting pulse is long gone, because still $t \approx \tau_d$. At a long time, $t = 196$ fs $\geq \tau_d$, the relaxation takes its course, the fields decay and yet again change their spatial distribution.

All of these distributions are radically different from the steady-state distribution obtained by the *independent* method of Refs. [2,3] for the same carrier frequency, shown in Fig. 3 (left panel). This difference is due to the fact that the pulse duration T is short, $T \lesssim \tau_d$. The driving pulse should be long enough, $T \gg \tau_d$, to obtain a dynamic distribution approaching the static one. We have verified this prediction by calculating the field distribution for a very long pulse shown in Fig. 3 (right panel). This

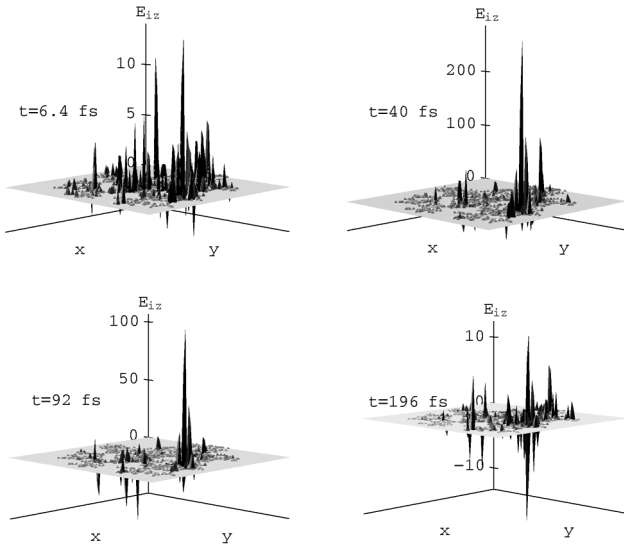


FIG. 2. Local fields $E_{iz}(t)$ for a 3d CCA cluster as functions of the spatial coordinates (x, y) for the moments of time indicated. The fields are summed over z for all monomers with the same (x, y) but different z to display the required 3d distribution on a plane figure.

distribution is indeed remarkably similar to the static one (cf. the two panels). This not only confirms our range of τ_d , but also independently verifies the validity and stability of our spatiotemporal solutions.

To interpret these results, we invoke the effect of giant fluctuations of local fields [4]. Though this effect has been predicted for steady-state excitation, it should take place also for the developed stage of femtosecond excitation ($t \gg \tau_\omega$) where the eigenmodes are already established. The distribution $P(I)$ of the relative local field intensity $I = E_i^2/E^{(0)2}$ scales as $P(I) \sim NI^{-\epsilon}$, where the critical exponent ϵ is very close to its binary-approximation value of $3/2$. With this distribution, an estimate for the maximum amplitude E_m of the local field that develops at one of the N monomers is $E_m/E^{(0)} \lesssim N^{1/[2(\epsilon-1)]} \sim 10^3$, in agreement with our calculated values. Hence, it is likely that in the course of the femtosecond excitation the giant fluctuations cause concentration of the local optical fields at hot spots and their colossal enhancement.

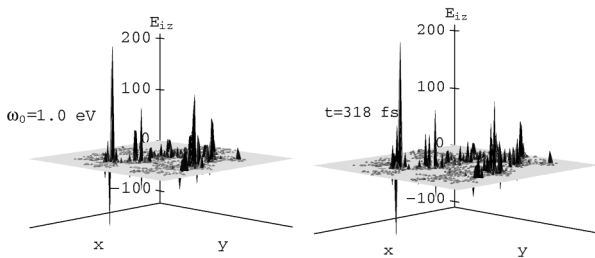


FIG. 3. Local fields presented similar to Fig. 2. Left panel: steady-state excitation with the carrier frequency $\omega_0 = 1$ eV. Right panel: Excitation with a pulse of $T = 500$ fs length.

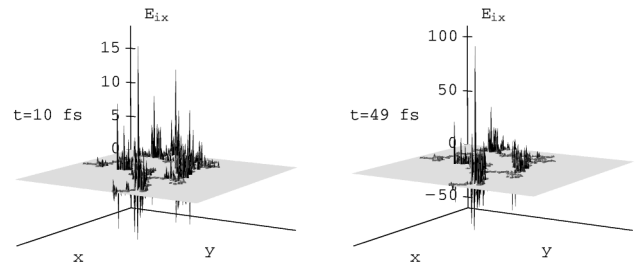


FIG. 4. Local fields $E_{iz}(t)$ for a 2D CCA cluster as functions of the coordinates (x, y) for the moments of time indicated. The exciting pulse has $\omega_0 = 0.75$ eV and $T = 30$ fs.

Regarding spatial correlations of the local field spikes, using our steady-state results [2] as a guidance, the spatial distribution and correlation functions of the local fields scale, i.e., depend only on the ratio r/R_c , where r is distance and R_c is the system's total size, for $R_c \gg r \gg l$. The minimum-scale length l is seen as the size of local field spikes. This size l in turn scales in the spectral variable as $l \approx R_m |R_m^3 X|^{-\lambda}$, where $\lambda \approx 0.25$ [2]. In the whole visible spectral region, $R_m^3 X$ is from -1 to -0.2 , so $l \approx R_m$. Hence, these spikes are always sharp, localized on a few monomers. Because of the scaling, larger clusters are expected to possess a similar behavior as long as their size is still less than the light wavelength. We will verify these predictions numerically elsewhere.

Given the universality of the giant fluctuations of local fields in fractal systems, we expect the ninth wave effect to exist in a wide class of fractal clusters, composites, and rough surfaces. Some manifestations of it may exist also in nonfractal random systems. We have confirmed a behavior qualitatively identical to the one described above for different individual 3D CCA clusters. We have also considered another fractal system, CCA clusters in 2D ($D \approx 1.4$), which can serve as a model for surface roughness. An example of results for such a cluster is shown in Fig. 4. At the initial stage ($t = 10$ fs), the local fields are excited at most monomers by a few first oscillations of the excited

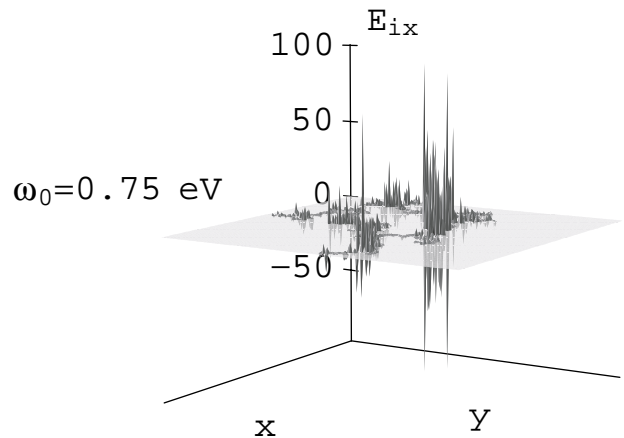


FIG. 5. Similar to Fig. 4, but obtained for a steady-state wave with the same carrier frequency $\omega_0 = 0.75$ eV.

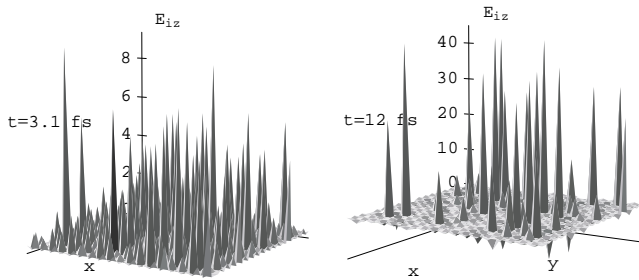


FIG. 6. Similar to Fig. 2 but for a random composite. The pulse parameters are $T = 10$ fs and $\omega_0 = 2.5$ eV.

field. Later ($t = 49$ fs), the single peak with the field enhancement $\approx 10^2$ dominates the distribution. These distributions are dramatically different from the distribution at the stationary excitation with the same frequency $\omega_0 = 0.75$ eV shown in Fig. 5.

A generally distinct behavior with some common properties is found for a nonfractal random composite (Fig. 6). Initially ($t = 3.1$ fs), the excitation of almost all monomers (inclusions) is pronounced, similar to fractal systems. However, at the maximum point ($t = 12$ fs), the field is not completely localized at just a few monomers in contrast to fractals. It is explained by much smaller fluctuations in nonfractal systems and much faster relaxation at $\omega_0 = 2.5$ eV where the composite absorbs.

The rich femtosecond behavior of local fields predicted above will manifest itself in a wide class of possible experiments. The hot spots will produce enhanced nonlinear responses. A contributing factor to it is that the femtosecond hot spot occurs under nondissipative conditions. This implies that it concentrates energy absorbed initially by many monomers similar to operation of an antenna (in contrast to steady-state conditions, where the hot spots are formed by the competition of the excitation and dissipation). In particular, the hot spots will dominate an enhanced Raman scattering and generation of third and higher harmonics for weakly saturating femtosecond pulses similar to the steady-state enhancement [19]. It is also feasible that a low-level femtosecond laser excitation can be combined with optical probe microscopy to track spatial details of the ultrafast local fields. With an increase of the pulse amplitude, optical saturation may modify the hot spots but is very unlikely to eliminate them. These hot spots will cause an enhanced production of femtosecond x-ray pulses and hot ions. The spatial distribution of local fields at a hot spot can be determined by means of x-ray or ionic microscopy using the laser-induced radiation of the system itself. The nanometer size of a hot spot makes it a prospective source

of x rays and ions for the purposes of microscopy and other applications.

I appreciate discussions with S. Manson and S. Faleev.

*E-mail address: mstockman@gsu.edu

Web site: www.phy-astr.gsu.edu/stockman

- [1] There had been a superstitious belief among old sailors that each ninth wave in a stormy sea is especially huge.
- [2] M. I. Stockman, Phys. Rev. Lett. **79**, 4562 (1997); Phys. Rev. E **56**, 6494 (1997).
- [3] M. I. Stockman, L. N. Pandey, and T. F. George, Phys. Rev. B **53**, 2183 (1996).
- [4] M. I. Stockman, L. N. Pandey, L. S. Muratov, and T. F. George, Phys. Rev. Lett. **72**, 2486 (1994).
- [5] P. Zhang, T. L. Haslett, C. Douketis, and M. Moskovits, Phys. Rev. B **57**, 15 513 (1998).
- [6] S. I. Bozhevolnyi, V. A. Markel, V. Coello, W. Kim, and V. M. Shalaev, Phys. Rev. B **58**, 11 441 (1998).
- [7] Z. Chang, A. Rundquist, H. Wang, M. Murnane, and H. C. Kapteyn, Phys. Rev. Lett. **79**, 2967 (1997).
- [8] S. Backus, C. G. Durfee, M. M. Murnane, and H. C. Kapteyn, Rev. Sci. Instrum. **69**, 1207 (1998).
- [9] I. P. Christov, M. M. Murnane, and H. C. Kapteyn, Phys. Rev. Lett. **78**, 1251 (1997).
- [10] F. L. Kien, K. Midorikawa, and A. Suda, Phys. Rev. B **58**, 3311 (1998).
- [11] M. M. Murnane, H. C. Kapteyn, S. P. Gordon, J. Bokor, E. N. Glytsis, and R. W. Falcone, Appl. Phys. Lett. **62**, 1068 (1993).
- [12] T. Ditmire, T. Donnelly, R. W. Falcone, and M. D. Perry, Phys. Rev. Lett. **75**, 3122 (1995).
- [13] L. Köller, M. Schumacher, J. Köhn, J. Tiggesbäumker, and K. H. Meiwes-Broer, Phys. Rev. Lett. **82**, 3783 (1999).
- [14] V. A. Markel, L. S. Muratov, and M. I. Stockman, Zh. Eksp. Teor. Fiz. **98**, 819 (1990) [Sov. Phys. JETP **71**, 455 (1990)]; V. A. Markel, L. S. Muratov, M. I. Stockman, and T. F. George, Phys. Rev. B **43**, 8183 (1991).
- [15] D. J. Bergman and D. Stroud, *Properties of Macroscopically Inhomogeneous Media*, in: Solid State Physics, edited by H. Ehrenreich and D. Turnbull (Academic Press, Boston, 1992), Vol. 46, p. 148.
- [16] P. Meakin, Phys. Rev. Lett. **51**, 1119 (1983).
- [17] M. Kolb, R. Botet, and J. Julienn, Phys. Rev. Lett. **51**, 1123 (1983).
- [18] P. B. Johnson and R. W. Christy, Phys. Rev. B **6**, 4370 (1972).
- [19] M. I. Stockman, V. M. Shalaev, M. Moskovits, R. Botet, and T. F. George, Phys. Rev. B **46**, 2821 (1992); V. M. Shalaev, M. I. Stockman, and R. Botet, Physica (Amsterdam) **185A**, 181 (1992).